5024 *Macromolecules* **2010**, *43*, 5024–5032
DOI: 10.1021/ma902805x

Macromolecules
ARTICLE

Annealing of Cocontinuous Polymer Blends: Effect of Block Copolymer Molecular Weight and Architecture

Joel R. Bell,[†] Kwanho Chang,[‡] Carlos R. López-Barrón,[§] Christopher W. Macosko,* and David C. Morse*

Department of Chemical Engineering and Materials Science, University of Minnesota, Minneapolis, Minnesota 55455. [†]*Present address: RTP Company, Winona, MN 55987. jbell@rtpcompany.com.*
[‡] *Present address: The Dow Chemical Company, Freeport, TX 77541. E-mail: KChang@dow.com.*
[§] *Present address: Department of Chemical Engineering, University of Delaware, Newark DE 19716*

Received December 22, 2009; Revised Manuscript Received April 20, 2010

ABSTRACT: Cocontinuous morphologies of polymer blends are thermodynamically unstable: they will coarsen when held above their glass or melting transition temperature. We have found that properly chosen diblock copolymers (bcp) can arrest coarsening during quiescent annealing. The effects of bcp on the cocontinuous morphologies of polystyrene (PS)/polyethylene (PE), PS/poly(methyl methacrylate) (PMMA) and PS/styrene-*ran*-acrylonitrile copolymer (SAN) blends were studied using scanning electron microscopy (SEM) and laser scanning confocal microscopy (LSCM) with image analysis. Bcp effectiveness was dependent on copolymer molecular weight, concentration, and asymmetry. Our interpretation emphasizes the role of bcp micelle creation and destruction as potential bottlenecks in the kinetics of interfacial adsorption of copolymer during mixing and of interfacial desorption during coarsening. In cases where adsorption and desorption appear to be facile, our results for the rate of coarsening are consistent with equilibrium predictions from self-consistent field theory for the dependence of interfacial tension upon copolymer asymmetry. We show that the coarsening of cocontinuous blends can provide a method to quantify the reduction in interfacial tension due to block copolymer addition, which is difficult to measure by conventional methods.

Introduction

Blending of immiscible polymers is an important route to high performance materials, often with synergistic improvements in properties.[1] When the blend composition is close to 50/50, cocontinuous morphologies can form with advantageous properties such as enhanced processability and mechanical properties,[2] static charge dissipation[3] and controlled moisture adsorption.[4] Cocontinuous blends tend to be less stable than blends with dispersed droplets, however, and coarsen rapidly and continuously during annealing.[2] A few studies, mostly with blends of polystyrene (PS) and polyethylene (PE), have shown that block copolymers can slow coarsening. Mekhilef et al.[5] found that the addition of styrene−(hydrogenated butadiene)−styrene (SEBS) triblock copolymer slowed the coarsening of cocontinuous morphologies in 50/50 PS/PE blends. In a more quantitative study, Veenstra et al.[6] found that 5% SEBS slowed coarsening 3-fold. Yuan and Favis[7] reported that adding 0.5% of a PS-*b*-PE diblock copolymer suppressed coarsening nearly completely while 7.5% SEBS was required to achieve similar stability. Galloway et al.[8] studied the effect of molecular weight and concentration of symmetric PS-*b*-PE bcp's and found that as little as 0.1% of bcp with an optimum molecular weight could completely suppress coarsening after an initial reduction in interfacial area.

Here we extend the experimental work of Galloway et al. and provide a more detailed theoretical interpretation of the results. We experimentally explore the role of block asymmetry, molecular weight and concentration in stabilization of cocontinuous morphology for another two polymer pairs with lower interfacial tension, PS/poly(methyl methacrylate) (PMMA) and PS/styrene-*ran*-acrylonitrile copolymer (SAN).

We note that an extremely low interfacial tension, and a correspondingly low rate of coarsening, could be obtained with symmetric copolymers at concentrations above the copolymer critical micelle concentration in either of two ways. Some systems of nearly symmetric copolymers of intermediate molecular weight can reach a very low equilibrium interfacial tension, in which the interfacial layer of adsorbed copolymer remains in equilibrium with a reservoir of micelles. Alternatively, in systems of longer copolymers, the interfacial coverage can be compressed above the equilibrium saturation coverage by the decrease in interfacial area during coarsening, thus driving the interfacial tension to zero, *if* copolymers are unable to desorb from the interface and reform micelles as interfacial area decreases. We discuss the expected implications of both of these scenarios, as well as a third in which, for sufficiently small copolymers, no micelles may form. We conclude that our results contain examples whose behavior is consistent with each of these three scenarios. In cases in which the evidence suggests that the interface remains in equilibrium with a reservoir of micelles, we infer values for interfacial tension from the observed rates of coarsening and compare these results to an equilibrium theory for the dependence of equilibrium interfacial tension upon copolymer asymmetry,[9] with encouraging results.

Experimental Section

Materials. Table 1 shows the properties of the blend components for these experiments. PS and high density PE (HDPE, Dow 4452N) were supplied by the Dow Chemical Company. Their low shear rate viscosities, at 0.1 rad/s and 170 °C, were

*To whom correspondence should be addressed. E-mail: (D.C.M.) morse@cems.umn.edu; (C.W.M.) macosko@umn.edu.

 Published on Web 05/05/2010

Table 1. Molecular Weight and Composition of Blend Components

material	M_n (kg/mol)	M_w/M_n	f_{PS}[a]	χN_{core}[b]	
PS	61	< 1.1			
HDPE (Dow 4452N)	18	5			
6K PS-*b*-PE	3−3	< 1.1	0.45	4[c]	
20−20K PS-*b*-PE	20−20	< 1.1	0.45	25[c]	
28−10K PS-*b*-PE	28.5−10.5	< 1.1	0.69	13[c]	
33−5K PS-*b*-PE	33−5	< 1.1	0.84	6[c]	
100K PS-*b*-PE	50−50	< 1.1	0.45	65[c]	
200K PS-*b*-PE	100−100	< 1.1	0.45	130[c]	
PS (Dow 685D)	150	1.8			
PMMA (Arkema V825N)	52	1.9			
FLPS	72	1.7			
SAN	71	1.6			
42K PS-*b*-PMMA	21−21	1.1	0.54	7[d]	0.9[e]
74K PS-*b*-PMMA	37−37	1.1	0.54		1.6[e]
100K PS-*b*-PMMA	50.6−47.6	1.1	0.55	17[d]	2.1[e]
160K PS-*b*-PMMA	80−80	1.1	0.54	27[d]	
260K PS-*b*-PMMA	130−133	1.1	0.53	44[d]	5.4[e]
900K PS-*b*-PMMA	450−450	1.1	0.54		18.8[e]

[a] Volume fraction of the PS block. [b] N_{core} is the total number of repeat units in the smaller block. [c] Using $\chi = 0.07$ (PS/PE).[10] [d] Using $\chi = 0.035$ (PS/PMMA).[16] [e] Using $\chi = 4.35 \cdot 10^{-3}$ (PS/SAN, Appendix).

nearly equal, 3200 and 3300 Pa·s, respectively. Viscosities were measured using a parallel plate rheometer (ARES, TA Instruments) in dynamic frequency. Symmetric (by weight) PS−PE diblock copolymers (PS-*b*-PE) with varying molecular weights, as well as two asymmetric 40 kg/mol (40K) PS-*b*-PE, were used. PS-*b*-PE was prepared by first synthesizing PS-*b*-PBD (polybutadiene) by anionic polymerization followed by selective hydrogenation. Details of the anionic polymerization, catalytic hydrogenation and characterization of the copolymers are described elsewhere.[10,11] Molecular weight and polydispersity of the polymers (shown in Table 1) were measured by gel permeation chromatography (GPC) using polystyrene standards. The volume fraction of the polystyrene blocks, f_{PS}, were measured by nuclear magnetic resonance.

PS (Dow 685D) and PMMA (Arkema V825N) are commercially available. Their low shear rate viscosities, at 0.1 rad/s and 220 °C, were both 11 000 Pa·s. The 42K, 74K, 100K, and 260K PS-*b*-PMMA were supplied by Polymer Source; information on their synthesis is given by Varshney et al.[12,13] The 900K PS-*b*-PMMA was supplied by Polymer Standard Services. The 160K PS-*b*-PMMA was synthesized at the University of Minnesota.[14]

Fluorescently labeled polystyrene (FLPS) and styrene-*ran*-acrylonitrile copolymer (SAN) were synthesized using free radical polymerization at 60 °C in toluene with azobis-(isobutyronitrile) as initiator.[15] 1% of a fluorescent monomer (anthracenylmethyl methacrylate) was used in the FLPS polymerization. The acrylonitrile content in SAN, measured by elemental analysis, was 19.3 mol %. The low shear rate viscosities of FLPS and SAN, at 0.01 rad/s and 200 °C, were 1500 and 2400 Pa·s, respectively.

Interaction Parameters. The last column of Table 1 contains estimates of the product χN_{core} of the Flory−Huggins interaction pararameter χ and the length N_{core} of the minority block of the copolymer for the PS/PE and PS/PMMA systems. Our interpretation of the results is that the kinetic barriers for micelle creation and dissolution are controlled primarily by this quantity. Values of N_{core} are given by $(1 - f_{core})M_n/M_o$, where f_{core} is the volume fraction of minority block and $M_o = \rho v N_A$ is the molecular weight of an effective monomer with reference volume v in a melt of mass density ρ. The same monomer reference volume was used to calculate all values of N_{core}. Values for PS/PE were calculated using $\chi = 0.07$ for a reference volume of 100 Å^3.[10] Values for PS/PMMA were calculated using $\chi = 0.035$ for PS/PMMA for a reference volume of 178 Å^3.[16]

The thermodynamics of the PS/SAN blends with PS-*b*-PMMA copolymers is both more complicated and less well characterized than the other two systems. Fowler et al.[17] observed miscibility in blends of PMMA and SAN with AN-content between approximately 9 and 33% by weight, and reported negative χ values for the PS−PMMA interaction. The compatibility between the SAN and PMMA blocks favors the presence of the copolymer in the SAN phase. Once there, we expect the equilibrium between micelle formation and dissolution to be governed by the interaction between the core block (the PS-block) and the SAN matrix; i.e. by $\chi_{PS/SAN}$. Because of the chemical similarity of PS and SAN, the value of $\chi_{PS/SAN}$ is expected to be smaller than that of PS−PE or PS−PMMA, but no reliable literature values are available for this parameter. As discussed in the Appendix, we have inferred an estimate $\chi_{PS/SAN} = 4.35 \times 10^{-3}$ from a measurement of the PS/SAN interfacial tension. We note that this estimate is only 50% above our estimate of the critical value of $\chi_{PS/SAN}$ required to induce phase separation in this blend. If this blend really is this near its critical point, however, we might not expect the relationship between χN_{core} and the magnitude of the kinetic barriers in this nearly miscible A/B blend with an A−C copolymer to be quantitatively the same as those in the other two much more strongly segregated A/B blends with A−B copolymers. These differences must be kept in mind when making quantitative comparisons of this system to the other two blends studied here.

Blend Preparation. PS/PE and PS/PMMA blends were prepared by mixing the components in a HAAKE batch mixer (HBI System 90 or Polylab OS, Thermo Electron Co.) using a 25 mL mixing bowl equipped with roller blades. To prevent thermal degradation, antioxidant (Irganox 1010, Ciba) was added at 0.2 wt %. The materials were dried under vacuum overnight. The dried materials, 20 g total, were added in one step, and mixed at 50 rpm (average shear rate = 25 s^{-1})[18] for 10 min at a temperature of 170 °C for PS/PE or 220 °C for PS/PMMA. The blends were then immediately removed from the mixer and plunged into a liquid nitrogen bath to quench the morphology. For PS/PE the blend composition was held constant at 50 wt % PS, while for PS/PMMA blends PS was 45 wt % to ensure the blend morphology was cocontinuous.[19]

50/50 FLPS/SAN blends were prepared in a recirculating, conical twin-screw extruder (Microcompounder, DACA Instruments) at 180 °C under nitrogen purge. Blending was performed at a screw speed of 100 rpm for 10 min. After mixing, blends were extruded from the mixer, quenched with water then cut into small pellets.

Annealing. After quenching the PS/PE blends, several pieces, ~2 mm thick, were annealed under quiescent conditions in the environmental chamber of our rheometer (ARES, TA Instruments). Samples were annealed for various time intervals at 170 °C under a nitrogen atmosphere then quenched using liquid nitrogen. PS/PMMA blends were annealed in a hydraulic press (Wabash). Small blend chunks were placed between Teflon sheets in a 25 mm diameter by 1 mm thick mold and then placed between the two heated metal platens. No pressure was applied. Samples were annealed for various time intervals at 220 °C. After annealing, cold water was flushed through the press platens to rapidly cool the samples below the glass transition temperatures of PS and PMMA; the cooling time (~1.25 min to ~100 °C) was taken into consideration for annealing time determinations. Pellets of FLPS/SAN blends were put in between two glass slides separated by 2 mm thick steel washers and then annealed in a Wabash hydraulic press at 200 °C for different time intervals. No pressure was applied in the sample to avoid any sample deformation. After annealing, the samples were plunged into water to stop the coarsening.

Scanning Electron Microscopy and Image Analysis. PS/PE samples were cryo-microtomed (Reichert UltraCut S Ultramicrotome) at −120 °C using a glass knife. Contrast between the phases was achieved by immersing each sample in toluene for 2 min to selectively remove the PS at the surface. PS/PMMA samples were microtomed at room temperature. Contrast between the phases was achieved by immersing each sample in cyclohexane at 40 °C for 4 min to selectively remove the PS at the surface. Care was taken to ensure that the extraction was deep enough to show the surface morphology, but shallow enough as to not expose other features of the sample interior.[20] Samples were then coated with 50 Å of platinum and imaged at 5 kV using scanning electron microscopy (SEM, JEOL 6500).

Since the size scale of the domains and depth of field in the micrographs made it difficult to accurately detect the interfaces using automated methods, the interfaces were manually traced for this analysis. The traced images were then scanned and each phase was filled in using graphic software (CorelDRAW). An analysis algorithm[20] was then used to determine the interface perimeter per unit area (Q) for each micrograph. For each set of conditions, 5 to 15 images were analyzed to determine the average Q. Assuming that the samples are isotropic, characteristic length for the cocontinuous morphologies is obtained by taking $1/Q$. It has been shown that phase size calculated using this 2D technique agrees with 3D results obtained using mercury porosimetry and X-ray microtomography as long as the phase size does not become too large.[22,21] Stereological corrections[22] may be used to correct errors in the large size region.[23]

Laser Scanning Confocal Microscopy and 3D-Image Analysis. FLPS/SAN samples annealed on glass slides were imaged, without further treatment, using laser scanning confocal microscopy (LSCM). For each sample a stack of about 100 2D images at different focal depths (z-position) was obtained. 3D images were rendered from the stacks, obtaining a triangular mesh depicting the blend interface. Details of the microscopy method and the image analysis can be found elsewhere.[15] The value of Q, in this case, was obtained by adding the surface area of all the triangles in the mesh and dividing by the sample volume.

Results

Effect of Block Copolymer Architecture. Figure 1 shows SEM micrographs of nonannealed and annealed 50/50 PS/PE blends without copolymer and with several 40K PS-*b*-PE copolymers of different compositions. All micrographs on the left represent blends quenched immediately after mixing and all micrographs on the right represent blends annealed for 15 min at 170 °C. Note that the scale bars differ for Figure 1, parts a and b. Figure 2 plots the characteristic length, $1/Q$, for these blends, showing the effect of bcp symmetry on suppression of coarsening. Even the most asymmetric copolymer, 33−5K, reduces the coarsening rate, but much less so than the more symmetric ones.

Effect of Block Copolymer Molecular Weight. Figure 3 shows the effect of annealing on 50/50 FLPS/SAN blends with and without 100K PS-*b*-PMMA. Micrographs on the left and right show blends after 5 and 60 min of annealing, respectively. Figure 4 shows the effect of the bcp molecular weight on $1/Q$ for the PS/PE (Figure 4a), PS/PMMA (Figure 4b), and FLPS/SAN (Figure 4c) blends. For the three systems, the block copolymer which proved to be the most effective in slowing the coarsening were 40K PS-*b*-PE for PS/PE, 42K PS-*b*-PMMA for PS/PMMA and for FLPS/SAN 100 and 260K PS-*b*-PMMA.

Effect of Block Copolymer Concentration. Figure 5 shows the effect of annealing on 45/55 PS/PMMA blends with varying concentrations of 100K PS-*b*-PMMA. All micrographs on the left represent blends annealed for 5 min at 220 °C and all micrographs on the right represent blends annealed for 60 min. Figure 6 gives plots of $1/Q$ vs annealing time for PS/PE, PS/PMMA and FLPS/SAN blends with varying concentrations of a copolymer that was effective at slowing coarsening. The plot in Figure 6a shows 50/50 PS/PE blends with 20−20K PS-*b*-PE, which was reported by Galloway et al.[8] The concentrations are 0.1, 0.3, and 1% PS-*b*-PE. The plot in Figure 6b shows 45/55 PS/PMMA blends with 100K PS-*b*-PMMA; concentrations are 0.1, 0.3, 1,

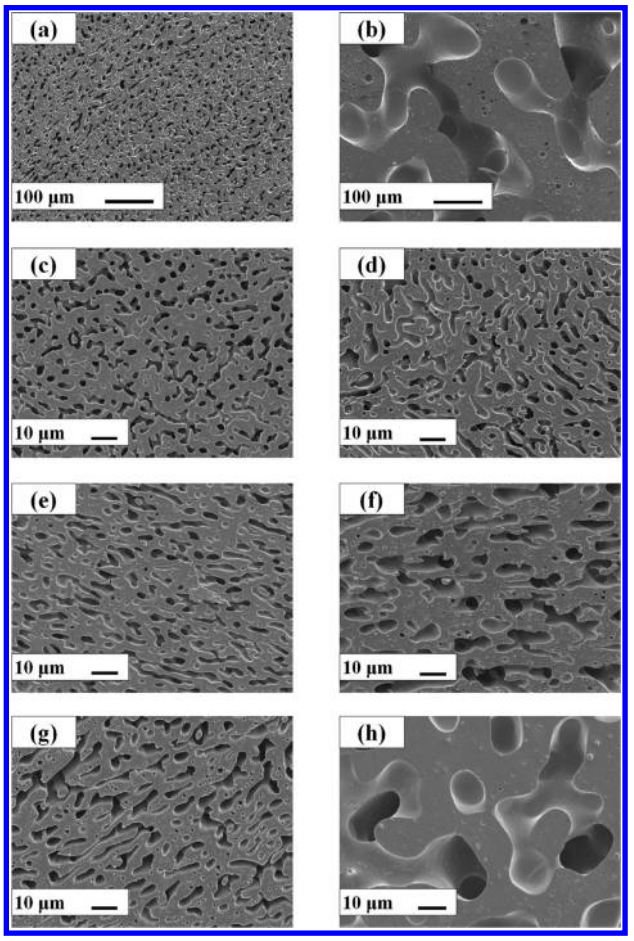

Figure 1. SEM micrographs of 50/50 PS/PE polymer blends with 1% 40K PS-*b*-PE with various block architectures, prepared by mixing at 50 rpm for 10 min at 170 °C. All micrographs on the left represent blends quenched immediately after mixing, while all micrographs on the right represent blends annealed for 15 min at 170 °C. Key: (a and b) no bcp; (c and d) 20−20K; (e and f) 28.5−10.5K; (g and h) 33−5K. (Note the scale bar = 100 μm for parts a and b and 10 μm for parts c−h).

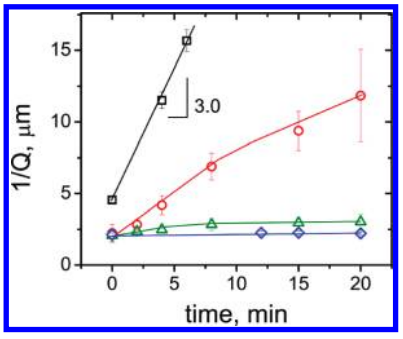

Figure 2. Plot of $1/Q$ vs annealing time at 170 °C for 50/50 PS/PE blends. Effect of block copolymer symmetry: blends with (□) no bcp, (○) 1 wt % 33−5K PS-*b*-PE, (△) 1% 28−10K PS-*b*-PE, and (◇) 1% 20−20K PS-*b*-PE. Lines are to guide the eye and error bars represent standard deviation.

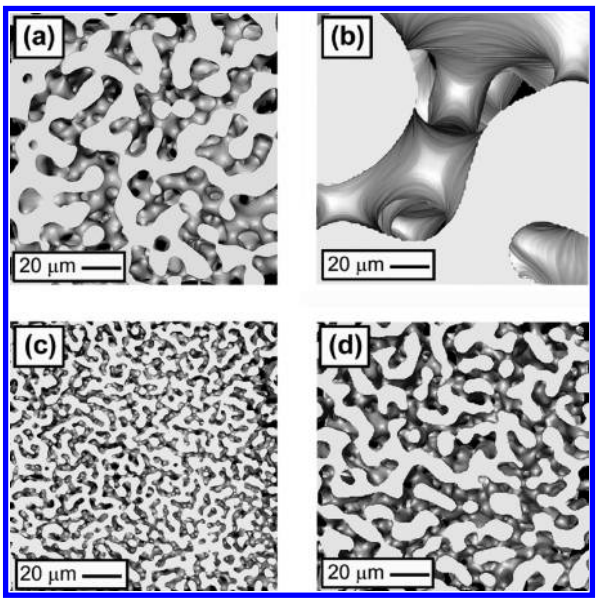

Figure 3. 3D rendered LSCM micrographs of 50/50 FLPS/SAN blends without bcp (a and b) and with 1% 100K PS-*b*-PMMA (c and d) prepared by mixing at 100 rpm for 10 min at 180 °C. Micrographs on the left represent blends annealed for 5 min after mixing, while micrographs on the right represent blends annealed for 60 min at 200 °C.

and 3% PS-*b*-PMMA. The plot in Figure 6c shows 50/50 FLPS/SAN blends with 100K PS-*b*-PMMA with concentrations 0.1, 0.5, 1 and 5% PS-*b*-PMMA. In the three plots an initial rapid coarsening is observed, followed by very slow or negligible coarsening for bcp concentrations <1%.

The coverage in number of bcp molecules per interfacial area, Σ, is a useful parameter for understanding the plateaus in Figure 6. Σ was estimated by

$$\Sigma = \frac{w_{bcp}\rho_{bcp}N_{av}}{QM_{\mathrm{n}}} \qquad (1)$$

where w_{bcp} is the weight fraction of bcp in the blend, ρ_{bcp} is the density of the bcp (0.855 g/cm^3 for PS-*b*-PE and estimated to be 1.0 g/cm^3 for PS-*b*-PMMA[24]), N_{av} is Avogadro's number, and M_{n} is the number-average molecular weight of the bcp. Equation 1 is based on the assumption that all the bcp added to the blends resides at the interface. The quantity Σ in eq 1 is thus an apparent interfacial coverage that we expect to be equal to or greater than the actual number of chains per area adsorbed to the interfaces. The maximum interfacial coverage Σ_{max} has been estimated by approximating the coverage of a saturated monolayer by the area per chain in the lamellar structure of the pure bcp. Lyu et al. reported Σ_{max} = 0.25 chains/nm^2 for the 20−20K PS-*b*-PE.[10] Using the scaling relation, $\Sigma_{max} \sim M_n^{-1/3}$, Σ_{max} is estimated to be 0.47 chains/nm^2, 0.18 chains/nm^2, and 0.15 chains/nm^2 for the 6K, 100K, and 200K PS-*b*-PE, respectively. For the 42K, 74K, 160K, 260K, and 900K PS-*b*-PMMA, Σ_{max} is estimated to be 0.159, 0.132, 0.102, 0.087, and 0.057 chains/nm^2, respectively, using Σ_{max} = 0.119 chains/nm^2 for the 100K PS-*b*-PMMA[25] and the same scaling relation. Table 2 shows Σ/Σ_{max} for the blends after mixing and after 60 min or from the average value of $1/Q$ when coarsening arrested.

The interfacial coverage results in Table 2 give insight into the plateaus in Figure 6. At 0.1% 40K PS-*b*-PE and 0.1% 100K PS-*b*-PMMA coarsening stops just at complete coverage, Σ/Σ_{max} = 1. For the higher concentrations of 40K PS-*b*-PE Σ/Σ_{max} = 1.2−1.3, which may also represent coarsening to just full saturation within the accuracy of this calculation.

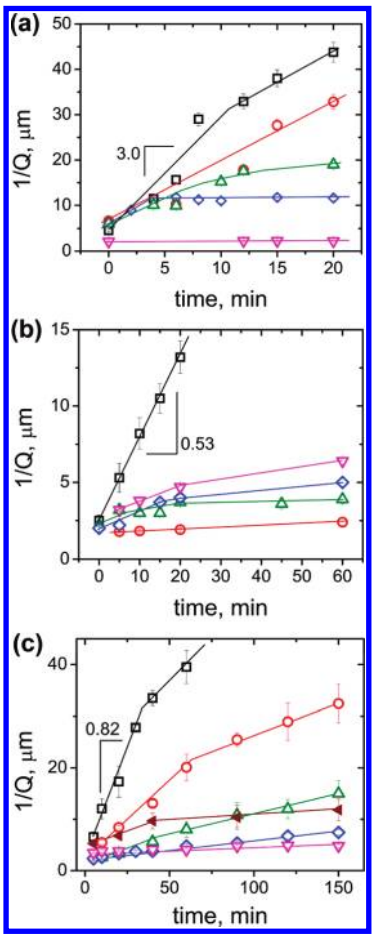

Figure 4. Plot of $1/Q$ vs annealing time for (a) 50/50 PS/PE, (b) 45/55 PS/PMMA and (c) FLPS/SAN blends: In (a): blends with (□) no bcp, (○) 1% 6K PS-*b*-PE, (△) 1% 200K PS-*b*-PE, (◇) 1% 100K PS-*b*-PE, and (▽) 1% 20−20K PS-*b*-PE [reference Galloway et al. 2005]. In (b): blends with (□) no bcp, (▽) 1% 260K PS-*b*-PMMA, (◇) 1% 160K PS-*b*-PMMA, (△) 1% 100K PS-*b*-PMMA, and (○) 1% 42K PS-*b*-PMMA. In (c): blends with (□) no bcp, (○) 1% 42K PS-*b*-PMMA, (△) 1% 74K PS-*b*-PMMA, (◇) 1% 100K PS-*b*-PMMA, (▽) 1% 260K PS-*b*-PMMA, and (▲)1% 900K PS-*b*-PMMA. Lines are to guide the eye and error bars represent standard deviation.

However, this concentration $\Sigma/\Sigma_{max} > 1$ also could indicate that some of the bcp is in micelles, perhaps formed during mixing. The fact that after mixing the 1% sample is already slightly above interface saturation supports micelle formation during mixing. All the compatibilized PS/PMMA blends, except the 0.1% 100K PS-*b*-PMMA, coarsen to Σ/Σ_{max} = 1.8 and some start at $\Sigma/\Sigma_{max} > 1$, again indicating micelle formation during mixing. The PS/PE blend compatibilized with 6K PS-*b*-PE has very high Σ/Σ_{max} values, pointing to relatively high solubility of bcp in the homopolymer. The same behavior was observed in the FLPS/SAN blend compatibilized 42K PS-*b*-PMMA.

Theoretical Considerations. The coarsening that we observe in these experiments is driven by interfacial tension. Several authors have predicted that the characteristic length scale, $1/Q$, of a cocontinuous structure should increase linearly with time[6,26,27]

$$\mathrm{d}Q^{-1}/\mathrm{d}t = c_1\Gamma/\eta \qquad (2)$$

where Γ is interfacial tension and η is polymer viscosity. Here c_1 is a dimensionless number that may depend upon the volume fractions of the two phases, the ratio of their viscosities, and

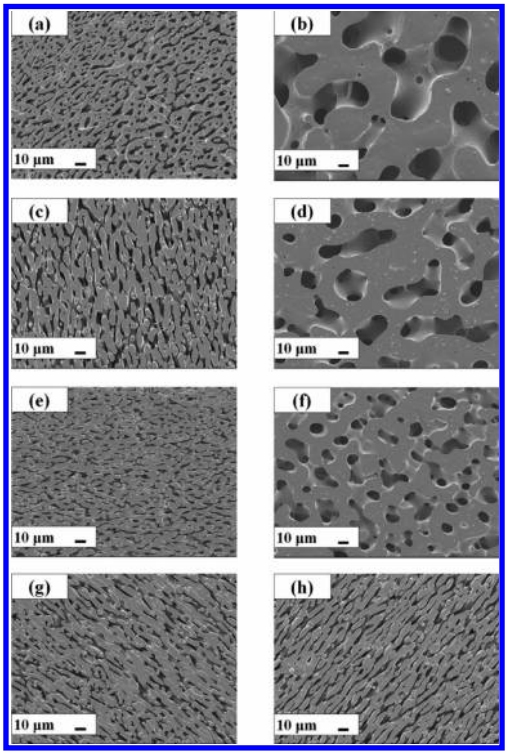

Figure 5. SEM micrographs of 45/55 PS/PMMA polymer blends with various amounts of 100K PS-*b*-PMMA, prepared by mixing at 50 rpm for 10 min at 220 °C. All micrographs on the left represent blends annealed for 5 min at 220 °C, while all micrographs on the right represent blends annealed for 60 min at 220 °C. Key: (a and b) have no bcp; (c and d) 0.1%; (e and f) 0.3%; (g and h) 1% PS-*b*-PMMA.

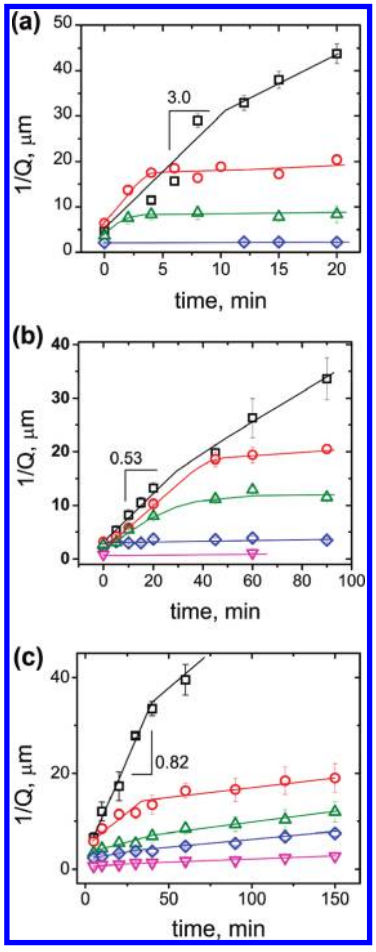

Figure 6. Plots of $1/Q$ vs annealing time for (a)50/50 PS/PE [reference Galloway et al. 2005], (b) 45/55 PS/PMMA, and (c) 50/50 FLPS/SAN blends. In part a: blends with (□) no bcp, (○) 0.1% 20−20K PS-*b*-PE, (△) 0.3% 20−20K PS-*b*-PE, and (◇) 1% 20−20K PS-*b*-PE. In part b: blends with (□) no bcp, (○) 0.1% 100K PS-*b*-PMMA, (△) 0.3% 100K PS-*b*-PMMA, (◇) 1% 100K PS-*b*-PMMA, and (▽) 3% 100K PS-*b*-PMMA. In part c: blends with (□) no bcp, (○) 0.1% 100K PS-*b*-PMMA, (△) 0.5% 100K PS-*b*-PMMA, (◇) 1% 100K PS-*b*-PMMA, and (▽) 5% 100K PS-*b*-PMMA. Lines are to guide the eye and error bars represent standard deviation. Note the difference in the time scales.

details of the interfacial geometry. This prediction follows from a simple balance of viscous stresses against capillary forces across curved interfaces.[26] If the structure coarsens in a self-similar manner (*i.e.*, if the only change in statistical geometry induced by coarsening is a change in characteristic length), and the interfacial tension remains constant, then c_1 should be independent of time, and should depend only upon volume fraction and viscosity ratio. This prediction is roughly consistent with the nearly linear increase of $1/Q$ with time that we, and others,[6,25−28] observed for immiscible blends in the absence of copolymer. Our observation of a decrease in dQ/dt at long times in the absence of block copolymer may indicate, however, that the coarsening is not perfectly self-similar over the time scale of the experiments[15,29] (see Figures 4 and 6).

In the presence of a copolymer some of the systems that we have studied exhibit an initial linear increase of $1/Q$ with time, followed by a dramatic decrease (or complete suppression) in the rate of coarsening. We assume that this dramatic decrease is the result of a decrease in interfacial tension caused by an increase in the interfacial concentration of adsorbed copolymer: As the system coarsens, the decrease in interfacial area tends to increase the concentration of adsorbed copolymer per unit area, and thus decrease the interfacial tension. If this process drives the interfacial tension to zero, the driving force for coarsening is removed, and coarsening ceases.

In its simplest form, the above argument assumes that any change in interfacial concentration during coarsening is solely a result of change in interfacial areas, but that no copolymer is transported to or from the interface during coarsening. This will be the case, however, only if there are significant kinetic or transport limitations to the adsorption or desorption of copolymer to or from the interface. In the absence of such limitations, coarsening would tend to force copolymer to desorb from the interface as the interfacial area decreased.

The opposite point of view would be to assume instead that there are no significant kinetic or transport limitations, and that the interface thus remains in diffusional equilibrium with a reservoir of dissolved copolymer and (generally) micelles. In this case, coarsening would tend to force copolymer to desorb in order to maintain a nearly constant interfacial concentration.

Before considering kinetic limitations in more detail, we discuss the expected behavior of the interfacial tension in true thermal equilibrium, along the lines of refs 9, 30, and 31. In equilibrium, the interfacial tension of a macroscopic interface decreases with increasing concentration of dissolved copolymer until the critical micelle concentration (cmc) is reached in one of the two coexisting phases. For concreteness, consider a mixture of A and B homopolymer containing A-B block copolymers in which the relevant cmc (i.e., the one that occurs at lower surfactant chemical potential) is that of the A phase. Once the concentration in the A phase exceeds this cmc, micelles form, and the equilibrium interfacial tension saturates to a value that is almost independent

Table 2. Normalized Interfacial Coverage, Σ/Σ_{max}, and Interfacial Tension, $c_1\Gamma$

	Σ/Σ_{max}[d]				normalized $c_1\Gamma$[c]	
Bcp	after mixing	after annealing[e]	$1/Q_0$[a] (μm)	$1/Q$[b] (μm)	initial	final
PS-*b*-PE (none)			4.6	43.8	1.00	
0.1% 40K (20−20)	0.3	1.0	6.4	20.4	0.80	0.05 ± 0.01
0.3% 40K (20−20)	0.6	1.3	3.7	8.4	0.42	0.00 ± 0.01
1% 40K (20−20)	1.1	1.2	2.1	2.2	0.00	0.00 ± 0.01
1% 40K (28.5−10.5)	∼1	1.3	2.1	3.0	0.01	0.01 ± 0.03
1% 40K (33−5)	∼1	6.2	2.2	11.8	0.16	0.13 ± 0.11
1% 6K	12.0	92	6.6	32.8	0.37	0.37 ± 0.05
1% 100K	1.8	3.2	6.4	11.6	0.24	0.01 ± 0.02
1% 200K	1.0	3.0	6.1	19.0	0.29	0.11 ± 0.08
PS-*b*-PMMA (none)			2.5	13.2	1.00	
0.1% 100K	0.2	1.0	3.2	10.3	0.75	0.08 ± 0.03
0.3% 100K	0.4	1.8	2.6	8.0	0.38	0.04 ± 0.01
1% 100K	1.1	1.8	2.2	3.6	0.13	0.01 ± 0.01
3% 100K	1.3	1.7	0.8	1.2	0.01	0.01 ± 0.00
1% 42K	1.6[g]	1.8	1.8[f]	1.9	0.02	0.02 ± 0.00
1% 160K	0.7	1.8	2.1	4.0	0.23	0.06 ± 0.01
1% 260K	0.9[g]	1.7	3.2[f]	4.7	0.18	0.08 ± 0.01
FLPS-*b*-SAN (none)			6.56[f]	17.32	1.00	
0.1% 100K	0.3[g]	0.8	5.8[f]	11.46	0.22	0.04 ± 0.02
0.5% 100K	0.9[g]	2.1	3.42[f]	5.50	0.11	0.04 ± 0.02
1% 100K	1.2[g]	2.4	2.31[f]	3.28	0.05	0.04 ± 0.01
5% 100K	1.6[g]	4.3	0.62[f]	0.94	0.02	0.01 ± 0.00
1% 42K	4.0[g]	18.1	4.46[f]	8.42	0.34	0.17 ± 0.04
1% 74K	1.6[g]	5.0	2.62[f]	3.25	0.15	0.09 ± 0.02
1% 260K	0.9[g]	1.1	3.4[f]	3.74	0.02	0.01 ± 0.00
1% 900K	0.6[g]	1.2	5.25[f]	6.77	0.15	0.02 ± 0.02

[a] Initial characteristic length (phase size). [b] Characteristic length after 20 min annealing. [c] Interfacial tension, $c_1\Gamma$, was normalized using $c_1\Gamma$ for the blend with no bcp. [d] Interfacial coverage. Assumes all bcp is at the interface. [e] Σ was calculated based on the specific interfacial area after 60 min or average area if coarsening arrested. [f] Characteristic length after 5 min annealing. [g] Calculated after 5 min of annealing to allow relaxation of anisotropy generated during the extrusion.

of concentration, which we will refer to as Γ_{cmc}. As discussed in ref 9, Γ_{cmc} is closely related to the difference between the free energy per interfacial area in the micellar state and that in a flat macroscopic interface. This free energy difference, and thus the equilibrium interfacial tension, depends strongly upon the composition of the copolymer and the structure of the micelles that it forms. Within a series of A-B diblock copolymers of varying composition f_A, for a given pair of homopolymers, Γ_{cmc} is expected to reach an almost vanishing minimum value at a value of f_A that corresponds to the "balance point" at which an interfacial monolayer of copolymer has a vanishing spontaneous curvature. In the idealized case of an interface between two homopolymers with the same molar volumes and the same statistical segment lengths, this balance point is $f_A = 0.5$.

We suspect that the most important kinetic limitation in this experiment is a limitation on the rates at which micelles can dissolve and reform. The rates at which micelles can dissolve into unimers, or form from a solution of dissolved unimers, can be described by an activated state theory analogous to the theory of homogeneous nucleation, as discussed by Semenov.[30] The relevant reaction coordinate is the number of copolymers in a micelle, and the activated state corresponds to a "critical nucleus" that is significantly smaller than the equilibrium micelle size. Semenov used strong stretching theory to estimate the barrier to the formation or dissolution of spherical copolymer micelles at the cmc. Semenov focused primarily on the barrier to micelle formation, but the barriers for formation and dissolution are equal at the cmc chemical potential, where the unimer and micelle states are in equilibrium. He found that the magnitude of the barrier to micelle formation depends primarily upon the product χN_{core}, and increases as $N_{core}^{4/3}$ with increasing core chain length. The predicted barrier becomes prohibitively large ($\gg 10kT$) for χN_{core} greater than a critical value of order 10. The implication is that only modestly segregated micelles can dissolve and reform rapidly enough to maintain equilibrium between an ensemble of micelles and a macroscopic interface.

Semenov's predictions are consistent with the results of our own work on measurements of interfacial tension in the presence of a block copolymer additive.[31] We found that very low equilibrium interfacial tensions were achievable reasonably rapidly with a series of low molecular weight diblock copolymers, for which $\chi N_{core} = 12$ approximately, but that transport of copolymer to the interface was several orders of magnitude slower for a symmetric copolymer with $\chi N_{core} = 25$, making it impossible for us to equilibrate systems containing the higher molecular weight copolymer. We attributed the slow transport of the longer copolymer to slow micelle dissolution.

The experiments presented here are sensitive to limitations on transport of copolymer to the interface only during the initial mixing process. The subsequent coarsening process is instead sensitive to the rate at which copolymer can be driven off the interface and reform into micelles. During coarsening, at concentrations above the cmc of the A homopolymer, a nonzero, nearly constant equilibrium tension Γ_{cmc} can be

maintained if copolymer can continuously desorb from the interface and reform into micelles. For the interface to stay in equilibrium with its surroundings at concentrations above the cmc, a constant concentration of dissolved free copolymers equal to the cmc must be maintained in the A phase, as well as a constant interfacial concentration. In equilibrium, any material that is driven off the interface must thus form micelles. Conversely, if micelles cannot form at the cmc chemical potential over experimentally relevant time scales, then upon coarsening the chemical potential within the interface can be driven above that of an equilibrated micellar solution, and so the interfacial tension Γ can be driven below Γ_{cmc}, potentially to zero.

The above discussion suggests three possible scenarios: (1) For sufficiently short copolymers, micelles may not form in equilibrium. (2) For somewhat longer copolymers, micelles may form, but micelle dissolution and creation may remain rapid. (3) For even longer copolymers, micelles will form, but micelle dissolution and creation can become very slow at the cmc. Which scenario will occur is controlled primarily by the value of the product χN_{core}, which controls both the thermodynamic and kinetic stability of a micelle. Each of these scenarios is discussed below in more detail:

Case 1: Sufficiently short copolymers do not form micelles. Diblocks with a B minority block that remain disordered in the limit of a pure copolymer melt, rather than forming an ordered phase, will generally also not form micelles in a dilute solution of copolymer in a A homopolymer matrix. In this case, we expect the equilibrium interfacial tension to decrease somewhat with increasing concentration of dissolved copolymer, but to remain nonzero at all concentrations. Also, because transport is not limited by slow micelle creation and dissolution, we expect copolymers to be able to desorb as the interfacial area decreases, and thereby maintain the nonzero equilibrium interfacial tension of an interface in equilibrium with a solution of molecularly dissolved copolymer. In this case, we thus expect *continuous coarsening at a nearly constant rate somewhat lower than that observed in the absence of copolymer*. We also expect that the apparent interfacial coverage could greatly exceed unity, i.e. $\Sigma/\Sigma_{max} \gg 1$.

Case 2: For somewhat higher molecular weight copolymers, there will exist a range of parameters in which micelles form, but micelle dissolution and formation may remain facile. Semenov's theoretical estimates,[30] and our experience with interfacial tension measurements,[31] suggest this will occur in (roughly) the range $\chi N_{core} = 10-20$. In this case, at concentrations above the cmc, the interface can remain in equilibrium, and so will maintain a nearly constant equilibrium interfacial tension Γ_{cmc}. Coarsening should proceed at a nearly constant rate that is independent of concentration above the cmc, but that depends upon the composition of the copolymer. Because Γ_{cmc} becomes very small for nearly balanced copolymers, this rate of coarsening may be very slow (perhaps immeasurably so) for such copolymers. In this case, we also expect that, if enough copolymer is added to system to cover the interfacial area generated during mixing, the interfacial tension should reach Γ_{cmc} during the mixing process, since transport to the surface is also not limited by slow micelle dissolution. We do not expect diffusion limitations to be important while the system is being subjected to intense mixing. We thus expect to observe a *nearly constant rate of coarsening starting from immediately after mixing ceases, but at a rate much lower than case 1* and even near zero for nearly balanced copolymers.

Case 3: For sufficiently strongly segregated micelles ($\chi N_{core} \gg 20$), rates of spontaneous micelle dissolution and reformation will become negligible at the equilibrium cmc. During mixing, this could limit the amount of copolymer delivered to the surface, and thus could result in a subsaturated interface with $\Gamma > \Gamma_{cmc}$ when mixing ceases. These samples will then coarsen until the interface saturates (as discussed above). During coarsening, copolymer will be stuck in the interface allowing the interfacial tension to be driven to zero by the coarsening process. This scenario could thus lead to a *measurable initial rate of coarsening*, even for nearly balanced copolymers, followed by a *dramatic decrease in the rate of coarsening* as the interfacial tension approaches zero.

Discussion of Results. There is some evidence for all three of the above scenarios in the coarsening experiments with PS/PE, PS/PMMA, and FLPS/SAN systems. We first consider the data for PS/PE systems.

The behavior of the 6K symmetric copolymer (Figure 4a) appears to be consistent with that expected in scenario 1: This system coarsens continuously at a rate slightly less than that of the system with no copolymer. At $\chi N_{core} = 4$, this symmetric copolymer is actually disordered and thus not expected to form micelles.

In the PS/PE systems, all of the 40K copolymers (Figure 2) exhibit behavior that appears to be consistent with scenario 2. All three systems exhibit a coarsening rate that is much lower than that obtained in the absence of copolymer. The rate of coarsening is easily measurable only for the 33K−5K copolymer, which is the most asymmetric of these three copolymers, for which we expect the highest value of Γ_{cmc}. We show below that the rates of coarsening for these systems are consistent with the values of Γ_{cmc} predicted from equilibrium self-consistent field theory (SCFT). One potential problem with this interpretation is the fact that our estimate of a value of $\chi N_{core} = 25$ for the 40K symmetric copolymer, using literature values for χ, is similar to our estimate of the same quantity for the PI/PDMS copolymer that was found to exhibit very slow transport to the interface in ref 31. Our proposed interpretation thus requires us to assume either that limitations on micelle dissolution and formation have a significant effect on this experiment only at somewhat higher values of χN_{core} than those at which they dramatically suppress transport in a macroscopic interfacial tension measurement, or that there is a significant uncertainty in the literature value of χ in one of these systems.

The behavior of the 100K and 200K symmetric PS-*b*-PE copolymer (Figure 4a) appear to be consistent with the predictions of scenario 3: Both exhibit initial coarsening followed by a saturation of the characteristic length $1/Q$.

Next, we consider our results for symmetric PS/PMMA polymers, shown in Figure 4b. All four symmetric PS/PMMA copolymers (42K, 100K, 160K, and 260K) yielded slow coarsening. The simplest explanation of this, by analogy with the explanation given above for the PS/PE systems, is that all of these systems are exhibiting scenario (2), micellization with facile micelle creation and dissolution. Our estimates of $6 < \chi N_{core} < 25$ for the 42K, 100, and 160K polymers are all less than or equal to our estimate for the symmetric 40K PS-*b*-PE polymer, which exhibited similar behavior. Our estimate of $\chi N_{core} = 44$ for the 260K PS/PMMA copolymer is, however, significantly higher than that of the 40K PS-*b*-PE copolymer, forcing us to (again) revise upward our estimate of the range of values of χN_{core} over which scenario 2 can be obtained.

Finally, three of the block copolymers used in the PS/PMMA blend (42K, 100K, and 266K PS-*b*-PMMA) and two more (74K and 900K PS-*b*-PMMA) were used to compatibilize the FLPS/SAN blend. The observed behavior in the

FLPS/SAN system can again be rationalized with the three scenarios discussed above: Scenario 1 with 42K and 74K PS-*b*-PMMA, scenario 2 with 100K and 260K PS-*b*-PMMA and scenario 3 with 900K PS-*b*-PMMA. The most effective compatibilizer for this blend was the 260K PS-*b*-PMMA (Figure 4c), in contrast to 42K PS-*b*-PMMA for the PS/PMMA system. At a qualitative level, the fact that higher molecular weight PS-*b*-PMMA copolymers are required to obtain scenarios 2 and 3 in this system than in the PS/PMMA blends is consistent with the fact that the PS−SAN core−matrix interaction parameter is much smaller than the PS−PMMA interaction parameter. Quantitatively, however, this difference in molecular weights is not as large as we would expect based on our estimates of the relevant χ parameters: Using $\chi = 4.35 \times 10^{-3}$ yields $\chi N_{core} = 2.1$ and 5.4 for the 100K and 260K PS-*b*-PMMA in SAN which appear to follow scenario 2, and $\chi N_{core} = 18.8$ for the 900K PS-*b*-PMMA that appears to follow scenario 3. These values can be compared to the range $\chi N_{core} = 6-44$ for the 42K−250K PS-*b*-PMMA copolymers in PMMA that all appeared to exhibit scenario 2. These quantitative differences may be the result of other differences between the PS/SAN blends and the other two systems, as already noted.

The block copolymers used for the concentration study (Figures 5 and 6) are all expected to follow scenario 2, i.e., coarsen at a constant rate that is controlled by the interfacial tension above the cmc. If there is enough copolymer to cover all of the interfaces at the end of mixing, they all should coarsen at the same rate, independent of the concentration. The normalized interfacial tension results in Table 2 for those systems are in reasonable agreement, supporting scenario 2.

Taken as a whole, the data remains broadly consistent with our proposed interpretation if we assume that the crossover between scenarios 2 and 3 occurs somewhere near $\chi N_{core} = 50$ in the strongly segregated PS/PE and PS/PMMA blends.

Comparison to Equilibrium SCFT. The above discussion suggests that the interfaces in the PS/PE blends with 40K PS-*b*-PE copolymer are probably in equilibrium with a reservoir of micelles. To test this idea, we have attempted to compare the values of normalized interfacial tension Γ/Γ_{max} that we inferred for the three different 40K copolymers to values predicted by equilibrium self-consistent mean field theory (SCFT).

Our analysis of these systems makes use of an approximation for Γ_{cmc} that was introduced in eq 21 of ref 9, in which Γ_{cmc} is expressed as a function of the elastic parameters of a saturated monolayer. All of our calculations use an interaction parameter of $\chi = 0.07$, and an average statistical segment length of $b = 6$ Å defined for a reference volume of $v = 135$ Å^3. All SCFT calculations have used monodisperse PE polymer with $N = 642$ (corresponding to the experimental value $M_n = 18$ kg/mol and $\rho = 0.78$ g/cm^3 for PE), and a monodisperse PS homopolymer with $N = 586$ (corresponding to $M_n = 61$ kg/mol and $\rho = 0.97$ g/cm^3 for PS). We used eq 21 of ref 9, to calculate Γ_{cmc} as a function of copolymer composition for several hypothetical series of copolymers in which we keep the core block size fixed and vary the corona block size. The three curves shown in Figure 7 are the results of a series of SCFT calculations of the Helfrich elastic parameters as functions of copolymer composition, in which the size of the PE block in each series was taken to be equal to the size of the minority block of one of the three 40K PS-*b*-PE copolymers that we studied experimentally. The single solid dot on each of the three curves marks the experimental value of f_{PE}, and is thus the predicted value for one of the three systems. Each of the three curves has a balance point at which Γ_{cmc} vanishes, which is the composition at which the spontaneous curvature vanishes for a copolymer with the specified core block size. The composition of the balance point is approximately $f_{PE} = 0.45$ for all three block sizes. Note that the 20−20K ($f_{PE} = 0.55$) and 28.5−10.5K ($f_{PE} = 0.31$) bcps fall on either side of the balance point, but remain close enough to the balance point to yield very low predicted values of $\Gamma_{cmc}/\Gamma_0 = 0.03-0.04$. The experimental values of Γ_{cmc}/Γ_0, shown as open squares in Figure 7, are even lower. The predicted value of $\Gamma_{cmc}/\Gamma_0 = 0.23$ for the 33−5K bcp is also slightly higher than the observed value of 0.16. We conclude that the data is broadly consistent with these predictions. 20−20K ($f_{PE} = 0.55$) and 28.5−10.5K ($f_{PE} = 0.31$) bcp fall on either side of the balance point, but are still close enough to produce appreciable reductions in Γ (see Table 2). The 33−5K bcp falls farther away from the balance point, but also shows some reduction in Γ. This would suggest that the shape of the quadratic is fairly broad for this system. Qualitatively, the theory appears to agree favorably with PS/PE experimental results.

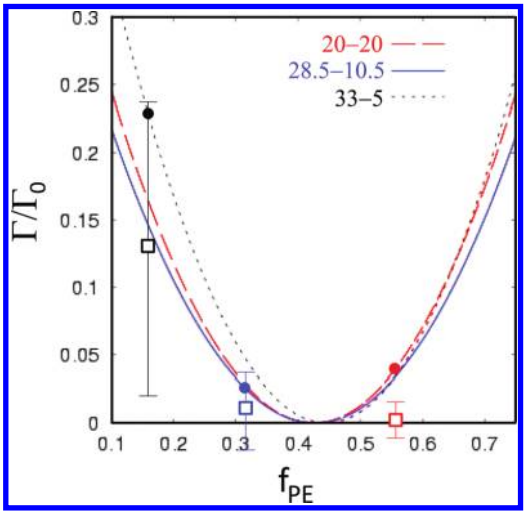

Figure 7. Interfacial tension (Γ) reduction vs volume fraction of PE block (f_{PE}) in PS-*b*-PE in the PS/PE system calculated from ref 9. At particular f_{PE} values the calculations (closed circles) can be compared to the experimental data (open squares) from Table 2 for the three 40K block copolymers with different symmetry.

Conclusions

The coarsening during annealing of cocontinuous polymer blends was measured via SEM and LSCM with image analysis. For all three systems studied here, i.e., PS/PE and PS/PMMA and FLPS/SAN, symmetric diblock copolymers of intermediate molecular weight were found to be most effective at stopping coarsening. The results were consistent with the theory proposed here in which three scenarios are expected, namely (1) poor compatibilization with short block copolymers due to its rapid desorption from the decreasing interfacial area during coarsening, (2) good compatibilization with intermediate size copolymers due to establishment of an equilibrium between desorption and micelle formation, and (3) initial fast coarsening followed by an abrupt stop of coarsening with sufficiently large copolymers, due to an incapacity of these to be transported to the interface and to desorb from it. Scenario 3 can also lead to good compatibilization if mixing can drive enough block copolymer into the blend interface.

The coarsening rate of cocontinuous blends can be used to quantify reduction of interfacial tension due to the addition of block copolymer. This is a difficult property to measure by the

usual pendant or spinning drop methods since it can take many hours for block copolymers to diffuse the typical distances required to reach equilibrium in these samples.[32] The interfacial tension reduction determined from coarsening measurements are consistent with values calculated by SCFT. In addition to being a class of multiphase polymer materials of practical importance, cocontinuous blends provide valuable insight into the thermodynamics and dynamics of block copolymers.

Acknowledgment. This work was supported by the MRSEC Program of the National Science Foundation under Award Number DMR-0212302, by the National Science Foundation under Award Number DMS-0352143, by a University of Minnesota Doctoral Dissertation Fellowship, and by a 3M Fellowship. Parts of this work were carried out in the Minnesota Characterization Facility which receives partial support from NSF through the NNIN program.

Appendix: Estimation of $\chi_{PS/SAN}$

We have tried to estimate $\chi_{PS/SAN}$ from the interfacial tension of the FLPS/SAN blend. We measured $\Gamma = 0.86$ mN/m at 200 °C using two methods: the breaking thread method and a rheological method.[29] Using the Helfand Tagami (HT) equation[33]

$$\Gamma = kTb\sqrt{6\chi}/v$$

where $v = 185$ Å^3 is the volume of a styrene repeat unit at 200 °C[24,34]and $b = 0.67$ is the statistical segment length, yields $\chi_{PS/SAN} = 2.2 \times 10^{-4}$. We consider this estimate implausible, however, because it can be shown that these two polymers would be miscible if χ were this low. We estimate a critical value for phase separation of $\chi_c = 3 \times 10^{-3}$ for this blend by treating it as a symmetric blend of two components with equal values of N_w and taking $\chi_c = 2/N_w$, while using $M_n = 70$K, $M_0 = 104$, $N_n = 673$ and $N_w/N_n = 1.7$ for both components. Here, we take polydispersity into account by noting that the spinodal curve of a blend of two polydisperse polymers is well approximated by using weight-averaged molecular weights in the Flory−Huggins theory,[35] and assuming an equimolar critical composition by symmetry.

The apparent failure of the Helfand−Tagami theory for our system can be understood by noting that this theory is valid only for strongly immiscible polymers, $\chi \gg \chi_c$, while the true interfacial tension vanishes at the critical point. To explain our data, we must thus either dismiss our measurement of the interfacial tension, or assume that this system is quite near its critical point. Using the empirical relation[36,37] $\Gamma/\Gamma_\infty = 1 - (\chi_c/\chi)^{2/3}$, in which $\Gamma_\infty(\chi)$ is the Helfand-Tagami prediction for infinite molecular weight, we obtain an estimate $\chi = 4.35 \times 10^{-3}$, or $\chi/\chi_c = 1.45$.

References and Notes

(1) Paul, D. R.; Bucknall, C. B. Introduction. In *Polymer Blends*, Paul, D. R., Bucknall, C. B., Eds.; John Wiley and Sons: New York, 2000; pp 1−14.
(2) Potschke, P.; Paul, D. R. *J. Macromol. Sci.* **2003**, *C43*, 87.
(3) (a) Lubrizol, Stat-Rite Conductive Polymers, The Lubrizol Corporation Technical Publication. Copyright 2007. Accessed at http://www.lubrizol.com/EngineeredPolymers/ asp on Sept 25th, 2009. (b) Conductive Thermoplastics, RTP Company Technical Publication. Copyright 2005. Accessed at http://www.rtpcompany.com/ on Sept 25th, 2009.
(4) Hekal, I. M. *Desiccant entrained polymer*, U.S. Pat. 5,911,937, **1999**.
(5) Mekhilef, N.; Favis, B. D.; Carreau, P. J. *J. Polym. Sci., Part B: Polym. Phys.* **1997**, *35*, 293.
(6) Veenstra, H.; Van Dam, J.; De Boer, A. P. *Polymer* **2000**, *41*, 3037.
(7) Yuan, Z.; Favis, B. D. *J. Polym. Sci., Part B: Polym. Phys.* **2006**, *44*, 711.
(8) Galloway, J. A.; Jeon, H.; Bell, J. R.; Macosko, C. W. *Polymer* **2005**, *46*, 183.
(9) Chang, K.; Morse, D. C. *Macromolecules* **2006**, *39*, 7746.
(10) Lyu, S.; Jones, T. D.; Bates, F. S.; Macosko, C. W. *Macromolecules* **2002**, *35*, 7845.
(11) Bates, F. S.; Rosedale, J. H.; Bair, H. E.; Russell, T. P. *Macromolecules* **1989**, *22*, 2557.
(12) Varshney, S. K.; Hautekeer, J. P.; Fayt, R.; Jerome, R.; Teyssie, P. *Macromolecules* **1990**, *23*, 2618.
(13) Teyssie, P.; Fyat, R.; Hautekeer, J. P.; Jacobs, C.; Jerome, R.; Leemans, L.; Varshney, S. K. *Makromol. Chem., Macromol. Symp.* **1990**, *32*, 61.
(14) Macosko, C. W.; Guegan, P.; Khandpur, A. K.; Nakayama, A.; Marechal, P.; Inoue, T. *Macromolecules* **1996**, *29*, 5590.
(15) López-Barrón, C. R.; Macosko, C. W. *Langmuir* **2009**, *25*, 9392.
(16) Russell, T. P.; Hjelm, J.; Seeger, P. A. *Macromolecules* **1990**, *23*, 890.
(17) Fowler, M. E.; Barlow, J. W.; Paul, D. R. *Polymer* **1987**, *28*, 1177.
(18) Maric, M.; Macosko, C. W. *Polym. Eng. Sci.* **2001**, *41*, 118.
(19) Bell, J. R. *Cocontinuous Polymer Blends: The Role of Block Copolymer in Blend Morphology Evolution*. Ph.D. Thesis, University of Minnesota, 2007.
(20) Galloway, J. A.; Montminy, M. D.; Macosko, C. W. *Polymer* **2002**, *43*, 4715.
(21) Pyun, A.; Bell, J. R.; Won, K. H.; Weon, B. M.; Seol, S. K.; Je, J. H.; Macosko, C. W. *Macromolecules* **2007**, *40*, 2029.
(22) Underwood, E. E. *Quantitative Stereology*; Addison-Wesley: Reading, MA, 1970.
(23) López-Barrón, C. R.; Macosko, C. W. *J. Microsc.* Submitted for publication.
(24) Fetters, L. J.; Lohse, D. J.; Richter, D.; Witten, T. A.; Zirkel, A. *Macromolecules* **1994**, *27*, 4639.
(25) Russell, T. P.; Menelle, A.; Hamilton, W. A.; Smith, G. S.; Satija, S. K.; Majkrzak, C. F. *Macromolecules* **1991**, *24*, 5721.
(26) Siggia, E. D. *Phys. Rev. A* **1979**, *20*, 595.
(27) McMaster, L. P. *Adv. Chem. Ser.* **1975**, *142*, 43.
(28) Yuan, Z.; Favis, B. D. *AIChE J.* **2005**, *51*, 271.
(29) López-Barrón, C. R.; Macosko, C. W. *Soft Matter*, DOI:10.1039/B926191E.
(30) Semenov, A. N. *Macromolecules* **1992**, *25*, 4967.
(31) Chang, K.; Macosko, C. W.; Morse, D. C. *Macromolecules* **2007**, *40*, 3819.
(32) Morse, D. C. *Macromolecules* **2007**, *40*, 3831.
(33) Helfand, E.; Tagami, Y. *J. Chem. Phys.* **1972**, *56*, 3592.
(34) Brandrup, J.; Immergut, E. H.; Grulke, E. A. *Polymer Handbook*, 4th ed.; Wiley: New York; 1999.
(35) Yang, J.; Sun, Z.; Jian, W.; An, L. *J. Chem. Phys.* **2002**, *116*, 5892.
(36) Anastasiadis, S. H.; Gancarz, I.; Koberstein, J. T. *Macromolecules* **1988**, *21*, 2980.
(37) Helfand, E.; Bhattacharjee, S. M.; Fredrickson, G. H. *J. Chem. Phys.* **1989**, *91*, 7200.